Electronic transport in carbon nanotubes: From individual nanotubes to thin and thick networks

V. Skákalová,[1,*] A. B. Kaiser,[2] Y.-S. Woo,[1] and S. Roth[1]
[1]*Max Planck Institute for Solid State Research, Heisenbergstrasse 1, 70569 Stuttgart, Germany*
[2]*MacDiarmid Institute for Advanced Materials and Nanotechnology, SCPS, Victoria University of Wellington, P.O. Box 600, Wellington, New Zealand*

(Received 27 February 2006; revised manuscript received 1 May 2006; published 9 August 2006)

We measure and compare the electronic transport properties of individual multiwall carbon nanotubes (MWNTs) and individual single-wall carbon nanotubes (SWNTs), and SWNT networks of varying thickness. The thinnest SWNT networks, like the individual semiconducting SWNTs, show nonlinear current-voltage (*I-V*) characteristics at low temperatures with a current that can be modulated by a gate-source voltage. The overall temperature dependence of conductance in the transparent networks changes systematically as the thickness of the network increases and is consistent with hopping conduction. On the other hand, the thickest SWNT networks (freestanding film) show more metallic behavior: their *I-V* characteristics are linear with no gate-voltage effect, and a large fraction of their conductivity is retained at very low temperatures, consistent with tunneling through thin barriers separating metallic regions. We make a comparison with individual MWNTs, which in some cases show even greater retention of conductance at very low temperatures, but (unlike the thickest SWNT networks) no changeover to metallic temperature dependence at higher temperatures. The temperature dependence of conductance in individual MWNTs is consistent with a model involving conduction in the two outer shells.

DOI: 10.1103/PhysRevB.74.085403 PACS number(s): 73.63.−b

I. INTRODUCTION

Single-wall carbon nanotubes (SWNTs) are produced as a mixture of nanotubes with a variety of different structures (corresponding to different ways of rolling up a graphene sheet), some with metallic and others with semiconducting band structures.[1–3] The electronic transport properties of an individual SWNT therefore depend on the type of nanotube as well as the experimental configuration and conditions. Individual SWNTs between two electrodes can behave as molecular quantum wires,[4,5] showing ballistic conduction with coherent electron states extending between the two electrodes. At low temperature, sections of SWNT may act as small islands with charging energy sufficient to produce Coulomb blockade effects, in which conductance peaks are seen as gate voltage is varied in a field effect transistor (FET) configuration.[4,6] At higher temperatures where Coulomb blockade effects lessen, there is evidence for power laws of conductance as a function of temperature, and differential conductance as a function of applied voltage, that are in agreement with the theoretical predictions for tunneling into Luttinger liquids in the nanotubes.[7,8] For semiconducting SWNTs, it was found that a key role was played by Schottky barriers formed at the interface between semiconducting tubes and metal leads.[9,10] Nevertheless, it was possible to construct FETs from semiconducting SWNTs,[11,12] in some cases by eliminating the Schottky barrier.[5]

Individual multiwall carbon nanotubes (MWNTs) mostly show a metallic character in their electrical conductance[13,14] but with an increase of conductance as temperature increases. It was inferred that conduction in MWNTs takes place mostly in the outer shell,[15] but recent results reveal a substantial contribution from conduction in the second shell after carriers tunnel from the outer shell.[16] There is also evidence for unconventional one-dimensional behavior resembling that of a Luttinger liquid (LL) in individual MWNTs,[17] although similar behavior is expected for the unconventional Coulomb blockade model.[18] A transition from LL-like behavior to conventional Fermi liquid behavior was seen in individual MWNTs as a gate voltage (of either sign) was applied.[19,20] Very recently it was shown that, when a MWNT grows directly from a tungsten filament and is contacted by another tungsten filament at the other end, electron transport can occur through all the shells of the tube and the conductance greatly increases;[21] a conductance several hundred times the conductance quantum G_0 was reported for an MWNT of diameter 100 nm using this technique, indicating quasiballistic conduction in all shells.

Besides individual CNTs, networks of CNTs are also of great interest for applications. This is illustrated for thin transparent films of SWNTs by the construction of a flexible transparent FET device changing its performance due to mechanical deformation.[22] Another application[23] is an electric field-activated optical modulator (the optical analog of the field-effect transistor): the key to the operation of this device was control of the charge carrier density in the thin SWNT networks by an electrolyte "gate" potential. Various chemical sensors use the charge transfer between detected molecules and the thin SWNT network that changes the conductance of the network.[24–27] In an earlier paper,[28] we showed that the charge carrier density in thick SWNT networks can be varied by chemical treatment with different molecules (resulting in either physical or chemical interactions). We identified the systematic variations in the conductivity and its temperature dependence as well as far infrared (FIR) absorbance and Raman line energies of the SWNT networks resulting from these treatments.

The "spaghettilike" conductive freestanding films of SWNTs show some similarities to those formed by organic conducting polymers. For these thick SWNT networks, we pointed out[29] a remarkable similarity to the temperature de-

pendence of conductivity of organic conducting polymers and showed that the SWNT data followed a model of interrupted metallic conduction similar to that used to account for electron transport in a large number of conducting polymers.[30] The experimental observations confirmed that the metallic tubes carry most of the current in SWNT networks, and that the resistance is dominated (especially at low temperatures) by barriers separating metallic portions of the SWNTs.

In this work, we investigate electronic transport changes as more complex carbon nanotube networks are formed from the same source of SWNTs. We start with measurements on individual SWNTs or bundles of SWNTs through very thin SWNT networks of increasing thickness to a thick freestanding SWNT film. For comparison we also investigate individual MWNTs consisting of concentric nanotubes of much larger diameter. The properties measured are the current-voltage (*I*-*V*) characteristics (including gate-voltage dependence) and the temperature dependence of the conductance. Analyzing and comparing the transport properties of individual semiconducting and metallic SWNTs (or bundles) as the basic units of SWNT networks, we conclude that in the thinnest percolating networks the semiconducting tubes dominate resistance. Increasing the thickness of the SWNT networks, more metallic behavior is observed. In the paper we suggest interpretations of the observed phenomena.

II. EXPERIMENTAL

A. Individual and parallel SWNTs

Purified HiPCO SWNTs were purchased from Carbon Nanotechnologies, Inc. (Texas). These SWNTs were suspended in a 1% aqueous solution of sodium dodecyl sulfate (SDS) followed by sonification and a centrifuge process, and then dispersed onto the palladium (Pd) electrodes prepatterned using electron beam lithography on a highly doped Si substrate with a silicon oxide layer of 200 nm in thickness. The distance between the source and the drain electrode was approximately 0.8 μm. An apparently individual SWNT placed between the source and the drain electrode was selected by means of atomic force microscopy (AFM). Using an etching process, our group has previously made high-resolution transmission electron microscopy (HRTEM) observations on the same SWNT samples used for room-temperature transport measurements, finding that AFM could not distinguish an individual SWNT from two thin SWNTs in parallel.[31] In the present work, the current-voltage (I_D-V_{DS}) characteristics between source and drain electrodes, and the gate (transfer) characteristics (using the highly doped Si substrate as the bottom gate) of the individual or parallel SWNTs, were measured down to low temperatures applying the two-terminal measuring method.

B. SWNT networks of different thicknesses

SWNT thin networks of four different thicknesses were air-brushed on the surfaces of four glass and four Si/SiO_2 wafers so that each pair of glass and Si/SiO_2 wafers was covered with the same number of brush strokes of SWNTs suspended in water with SDS. The first pair of glass and Si/SiO_2 wafers (Net 1) was given two brush strokes (i.e., forward and back), with four brush strokes for the second pair (Net 2), six brush strokes for the third pair (Net 3), and eight brush strokes for the last pair (Net 4). All the samples were then rinsed in deionized water to remove the SDS from the wafer surfaces. The transparent networks of SWNTs form agglomerates of nanotube bundles containing many well-aligned tubes alternating with empty regions, as shown in Fig. 1. Therefore, it is difficult to define the thickness of these networks. Optical transmission was chosen as an appropriate method of averaging the structural irregularities and characterizing the thickness of various thin SWNT networks prepared on a glass substrate, using a UV-VIS/NIR Perkin-Elmer Lambda Spectrometer in the range of wavelengths from 1100 to 200 nm. The transmittance values at 1100 nm wavelength measured on our four transparent networks are given in Table I.

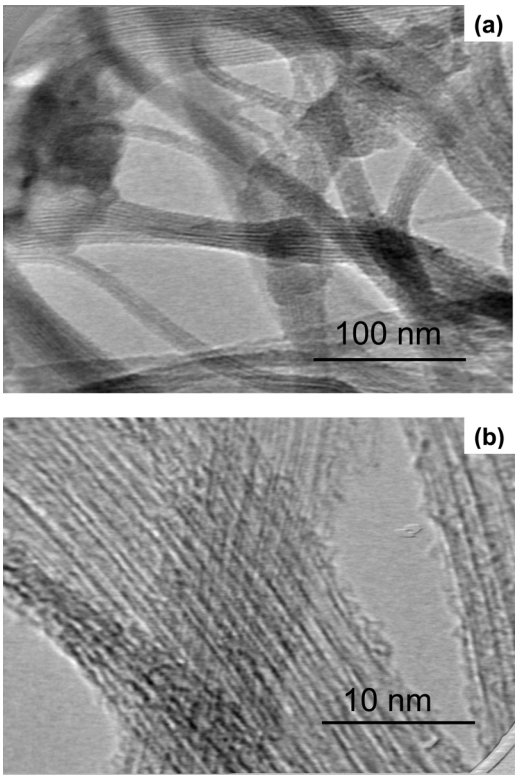

FIG. 1. An example of TEM images of our thin SWNT networks showing the morphology of the SWNT bundles (a), and at higher magnification, the SWNTs within a bundle (b).

A SWNT thick freestanding film was prepared from a suspension of SWNT in water with SDS by vacuum filtration through a membrane filter (0.4 μm pores). The thickness of the freestanding film obtained was 35 μm.

The electrical conductance of the SWNT freestanding film and of the four thin SWNT networks on Si/SiO_2 wafers was

TABLE I. Transmittance of transparent networks.

SWNT network	Net 1	Net 2	Net 3	Net 4
Transmittance (%)	95%	70%	50%	30%

measured by the four-probe method. Four chromium (20 nm thick)/gold (200 nm thick) strips of the same geometry were evaporated on top of all the samples, i.e., 1 mm distance between the central (voltage) strips. A constant current was applied during the temperature-dependence measurements from liquid helium temperature up to room temperature.

C. Individual MWNTs

Samples of multiwall carbon nanotubes (MWNT) grown by chemical vapor deposition (CVD) were fabricated by Infineon Technologies (Germany). For the four-probe electrical measurements, underlying Ti/Co contacts were deposited on the surface of Si/SiO_2 wafers and MWNTs were randomly adsorbed on top. Pd was then deposited by electroless deposition on top of the MWNTs following the procedure given in Seidel *et al.*[32]

III. RESULTS AND DISCUSSION

A. Individual or two or three parallel SWNTs

We start by presenting the electronic transport properties of individual SWNTs or two or three parallel SWNTs that are the basic units of the SWNT networks that we prepared. In Fig. 2 we show measurements of the current-voltage characteristics for two representative samples out of ten, a thin bundle of about three tubes (m-SWNT) showing metallic behavior, and a (possibly) individual tube (s-SWNT) showing semiconducting behavior.

The drain current I_D in the m-SWNT shown in the inset to Fig. 2(a) changes little with gate-source voltage V_{GS}, indicating metallic behavior, whereas that for s-SWNT shown in the inset to Fig. 2(b) is quenched for positive gate voltages V_{GS}, indicating *p*-type semiconductor behavior. The current-voltage characteristics of s-SWNT at low temperatures are markedly different from those of the metallic m-SWNT: there is an apparent threshold effect with only small currents flowing until the magnitude of V_{DS} exceeds 0.5 V, and the shape of the I_D-V_{DS} characteristics changes substantially as the temperature, T, increases. To characterize the conduction process in our SWNTs, we investigate the behavior of the current I_D as a function of V_{DS}, and low-field conductance G as a function of temperature in more detail.

Hunger *et al.*[33] studied electronic transport through thick bundles of SWNTs in which the metallic SWNTs dominate transport. They found that two different models, the Luttinger liquid theory as well as a nonohmic interfacial barrier approach, both fit their data sufficiently well. We explore the applicability of both approaches for our metallic SWNTs.

If the SWNT behaves as a Luttinger liquid, and there is a tunneling barrier between the electrode and the SWNT, the conductance in the ideal case will reflect the power-law behavior of the density of states in the Luttinger liquid, yielding power laws:[7,34]

$$I_{SD} = bV^{\beta} \quad (\text{for eV} \gg k_B T), \tag{1}$$

$$G = aT^{\alpha} \quad (\text{for } k_B T \gg \text{eV}), \tag{2}$$

where a and b are constants, e is the electronic charge, k_B is Boltzmann's constant, and V is the voltage across the tunneling barrier (i.e., the appropriate fraction of the drain-source voltage V_{DS} in the present experiment). The power-law exponents for a Luttinger liquid are related by

$$\beta = \alpha + 1. \tag{3}$$

Of course, these relations would be observed experimentally for the current between electrodes only if the transport across the SWNT-electrode barriers is independent of energy.[33]

The I_D-V_{DS} characteristics for m-SWNT in Fig. 3 show only a modest variation with temperature, consistent with the predominantly metallic character. Nevertheless, there is a significant nonlinearity in I_D as a function of drain-source voltage V_{DS} that is stronger at low temperatures, and there is evidence for power laws as a function of voltage (at larger voltages), as shown in Fig. 3(a), and as a function of temperature (at low voltages), as shown in Fig. 3(b).

Given that our experiment involves two tunnel junctions that will not be identical, we conclude that our values of 0.60 and 1.75 for α and β respectively from Eqs. (1) and (2) are in reasonable agreement with the Luttinger-liquid prediction, Eq. (3). Our value of the exponent α is similar to that ob-

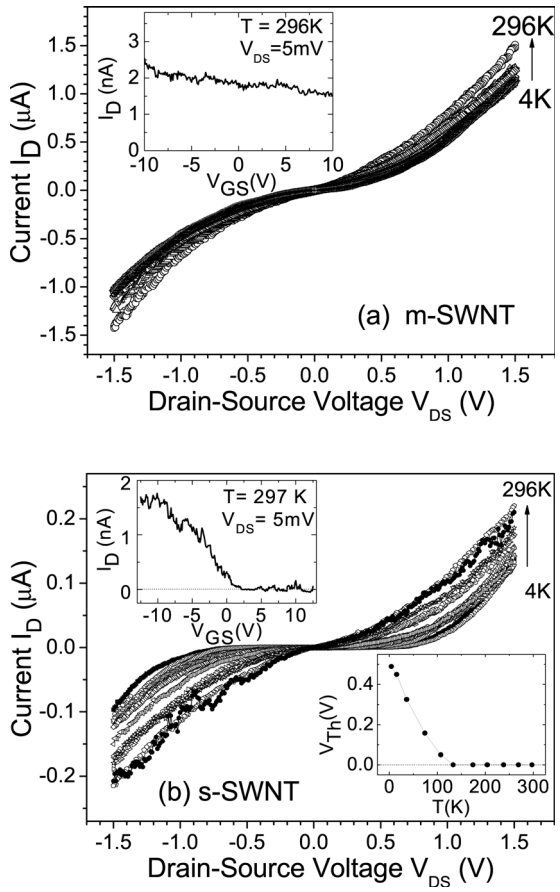

FIG. 2. Current-voltage ($I_D - V_{DS}$) characteristics of SWNTs at a range of temperatures between room temperature and 4 K: (a) m-SWNT (metallic type) and (b) s-SWNT (semiconductor type); the upper left insets (a) and (b) show examples of the dependence of the drain current I_D on gate voltage V_{GS}, while the lower right inset (b) shows the dependence on temperature of the threshold bias voltage V_T at which detectable current flows.

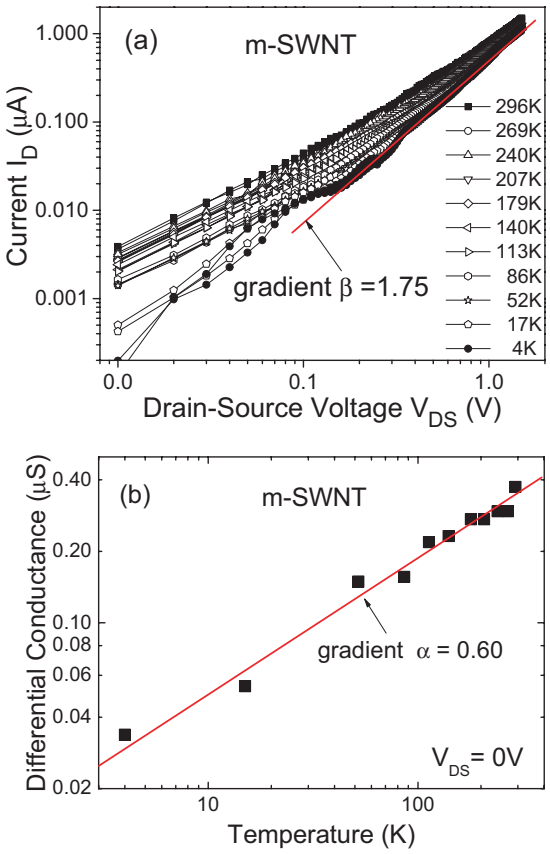

FIG. 3. (Color online) Power laws for metallic m-SWNT. (a) Drain current I_D as a function of drain-source voltage V_{DS} (using logarithmic scales) for temperatures ranging from 4 K to 296 K, showing the trend to a power law with exponent approximately $\beta = 1.75$ at higher voltages (measurements for increasing and decreasing voltage are shown for each temperature). (b) Conductance at zero bias as a function of temperature T (using logarithmic scales), showing approximate agreement with a power law with exponent $\alpha = 0.60$.

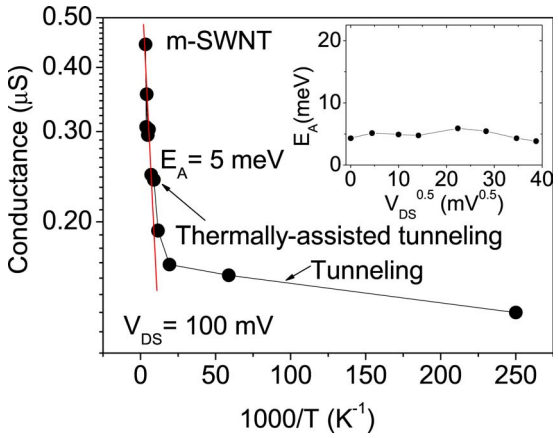

FIG. 4. (Color online) Conductance G at 100 mV (using a logarithmic scale) as a function of inverse temperature, showing two mechanisms: tunneling at low temperatures and activated behavior with energy $E_A = 5$ meV at high temperatures.

tained earlier[7] for end-contacted SWNTs. We note, however, that our configuration with the SWNT deposited on top of the electrodes would be expected to correspond more closely to the bulk-contacted case where the Luttinger liquid extends beyond the inner SWNT-electrode contact point; in this case, the values obtained for α lay in the range 0.3–0.4.[7] Similar power-law behavior can arise from an unconventional Coulomb blockade model,[18] so the interpretation in terms of Luttinger liquids is not necessarily unique.

Since Hunger *et al.*[33] found that transport in their large metallic bundles could equally well be accounted for by a model of temperature-dependent transport across interfacial barriers between the metallic SWNTs and electrodes, we have investigated this possibility for our m-SWNT sample. We observe that the small activation energy of 5 meV obtained from the high-temperature portion of our conductance Arrhenius plot (Fig. 4) is of similar size to their values at small bias voltages. However, our activation energies show little dependence on bias voltage (inset of Fig. 4), in contrast to their results. It therefore appears that the temperature dependence of transport in our m-SWNT sample does not arise from an interfacial metal-metal "resistivity-dipole" barrier (similar to a Schottky barrier) that they suggested for their large bundles, although thermally-assisted tunneling as temperature increases could give rise to the similar increase in conductance we observe at higher temperatures. The disagreement between the findings of Hunger *et al.*[33] and our results could originate from the fact that in the very thick SWNT bundles they studied, more intertube interactions will occur, and the large number of semiconducting tubes also present in the bundle will start to contribute to the transport when the bias increases. Our metallic bundle consists of two or three tubes only.

We consider now the semiconducting nanotube. Figure 5(a) shows the I_D-V_{DS} characteristics of the s-SWNT at various temperatures in log-log scale. At low temperatures and drain-source voltages below the critical threshold voltage, we identify no measurable current. [The threshold voltages plotted in the inset to Fig. 2(b) are essentially the values where the current is reduced below 10^{-5} μA as estimated from I_D-V_{DS} plotted in semilogarithmic scale.] There is a sharp decrease in current for low voltages and temperatures below 150 K. At larger temperatures the curves could be fitted by a power law in drain-source voltage, and even at low temperatures there is a trend towards similar behavior of the current at large values of the drain-source voltage V_{DS} with exponent $\beta = 3.3$. We do find a power-law dependence of conductance on temperature for the zero-bias conductance above 70 K, as shown in Fig. 5(b), but the exponent is $\alpha = 3.9$ (for a Luttinger liquid typically $\alpha < 1$), and the values of the exponents α and β do not satisfy the condition (3). This confirms that the s-SWNT is a semiconducting tube and not a Luttinger liquid.

On the other hand, one would expect that, at the metal contacts with ends of a semiconducting tube, two Schottky barriers will be formed and charged in opposite directions. Then the reverse barrier with respect to the applied electric field would always limit the current flowing in the circuit. This picture explains the large current blockade with the breakdown threshold at high-bias voltages ($V_{DS} \sim 0.5$ V at 4 K) observed in the I_D-V_{DS} characteristics of the s-SWNT

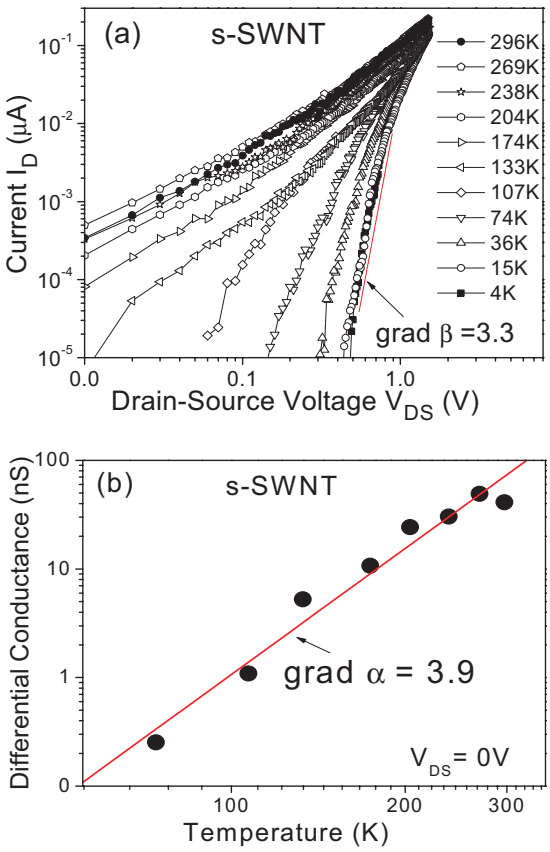

FIG. 5. (Color online) Power laws for semiconducting s-SWNT: (a) Drain current I_D as a function of drain-source voltage V_{DS} (using logarithmic scales) for temperatures ranging from 4 K to 296 K, showing approximate agreement with a power law with exponent β=3.3 for data above 500 mV at 4 K; (b) Zero-bias conductance G as a function of temperature (using logarithmic scales), showing approximate agreement with a power law with exponent α=3.9 for data above 70 K [as indicated in Fig. 5(a) the zero-bias conductance becomes too small to measure at low temperatures].

[Fig. 2(b)]. As the temperature increases, the threshold voltage is reduced as shown in the lower right inset of Fig. 2(b).

Figure 6 represents a conductance Arrhenius plot in the temperature region above 70 K. Below 70 K, the current is under the measurable limit. At the bias voltage V_{DS}=0.1 V, the activation energy is 29 meV. The inset of Fig. 6 shows how the activation energy changes as a function of the square root of the bias voltage. We see a decreasing dependence, nevertheless, slightly deviating from a linear one in a bias region several times larger than that reported in earlier studies.[33,35] The mechanism of electrons passing the barrier in reverse direction might be complex; however, the low values of the activation energies most likely reflect a process of thermally assisted tunneling, which is possible in the case of very thin Schottky barriers. We conclude that in the semiconducting SWNTs, the existence of Schottky barriers appears to explain the electron transport mechanism satisfactorily.

B. SWNT networks of different thicknesses

In this section, electrical properties of four thin SWNT networks are studied. They are characterized by the plot in

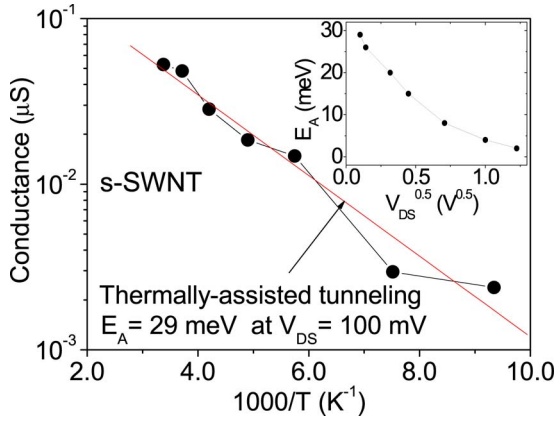

FIG. 6. (Color online) Conductance G at 100 mV (using a logarithmic scale) as a function of inverse temperature, showing a good agreement with activated behavior with activation energy E_A =29 meV.

Fig. 7 where the conductance per square changes with the optical transmittance of the thin networks. For comparison, the conductance per square value of a thick SWNT freestanding film is shown at zero transmittance in Fig. 7.

Figure 8 demonstrates the I-V characteristics of the four thin networks of SWNT with different thickness at liquid helium temperature and at room temperature. At low temperature [Fig. 8(a)], the thinnest networks show a nonlinear behavior similar to that of the individual s-SWNT [Fig. 2(b)], while linear plots characterize the thicker networks. At room temperature [Fig. 8(b)], some slight nonlinearity remains visible only for the thinnest network.

In a simple picture, we assume that two-thirds of all the nanotubes present in the sample are semiconducting. Therefore it is reasonable to expect that for diluted networks of SWNTs of a density slightly above percolation threshold, first semiconducting tubes form percolation paths. In the case of conducting networks, we deal with a complex series-parallel circuit (in contrast with the parallel circuit in a single bundle of SWNT) and therefore the metallic tubes would play a role only as interconnects between the semiconducting tubes that determine the semiconducting character of the to-

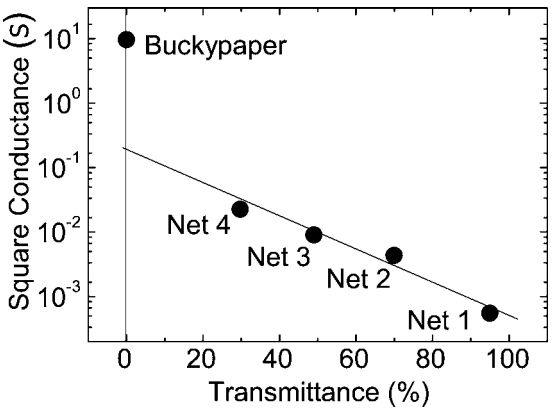

FIG. 7. Magnitudes of the square conductance for each sample showing the correlation with the optical transmittance at 1100 cm^{-1} for the transparent SWNT networks of different densities.

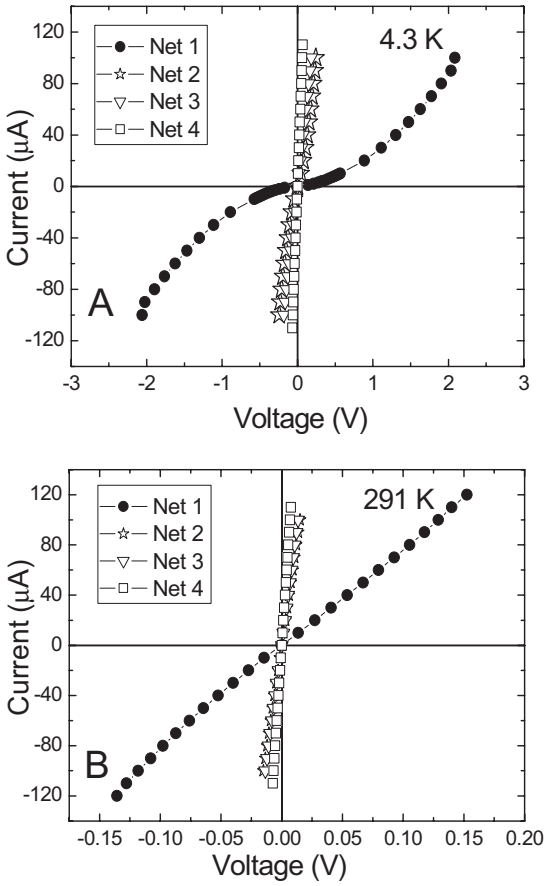

FIG. 8. $I_D - V_{DS}$ characteristics of thin SWNT networks Net 1 (thinnest) to Net 4 at 4.3 K (a) and 291 K (b).

tal conductance of a network. Schottky barriers are formed at the interface of the metal contacts as well as at the junctions of semiconducting and metallic tubes, similar to the case of the individual s-SWNT presented above. As the networks become denser, more and more percolating paths are formed by metallic tubes so that ohmic character of electron transport takes over.

We also demonstrate how the density of a network determines the quality of a field effect transistor (FET) device varying its properties from semiconducting towards metallic ones. The carrier channel of the FET device is established through the SWNT network separated from the bulk of the highly doped Si chip serving as a bottom gate by an insulating SiO_2 layer. Figure 9 shows the gate (transfer) characteristics of the networks with different values of optical transmittance at a temperature of 4.3 K and at 290 K. At room temperature, the "on-off" ratio of the device made of the highly transparent SWNT network (Net 1) is about 10 000, while for the denser network device (Net 4), the value is about 2.8. At low temperatures, conductance is realized more through the metallic tubes since the semiconducting tubes become insulating. Therefore, at 4.3 K, the "on-off" ratio decreases in both networks.

The set of curves in Fig. 10 shows the temperature dependence of the electrical conductivity of the thick and four thin SWNT networks, with conductivity $\sigma(T)$ normalized to its value near room temperature. A stronger decrease of the curves as T decreases is observed, as the layers get thinner. As discussed earlier,[28] the thick network shows clear signatures of metallic behavior: the conductivity remains large in the zero-temperature limit (more than 40% of the room-temperature conductivity), and there is a change to metallic sign for the temperature dependence above 240 K [a weak decrease in conductance $G(T)$ as temperature increases above 240 K].

In quasi-one-dimensional conductors in which carriers cannot circumvent defects or other barriers to conduction, a model of interrupted metallic conduction has been used to account for the mixed metallic/nonmetallic behavior observed in highly conducting polymers and in SWNT networks.[30] If the barriers between metallic regions are thin, a substantial conductance can still be seen in the zero-temperature limit (metallic behavior). As temperature increases, thermal fluctuations assist the tunneling and increase the conductance (yielding a nonmetallic sign for the temperature coefficient). At higher temperatures, the usual de-

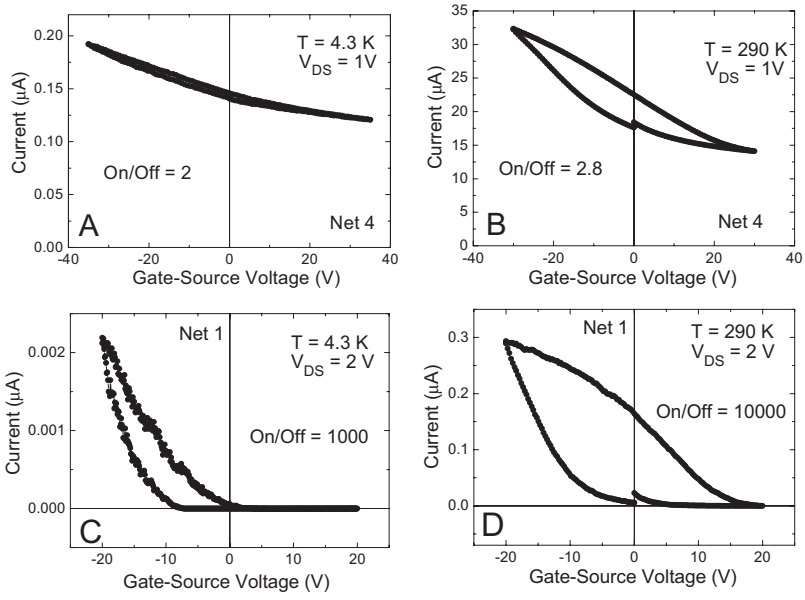

FIG. 9. The effect of a gate voltage V_{GS} on the current I_D of Net 4 at temperatures of 4.3 K (a) and at 290 K (b) and of Net 1 at temperatures of 4.3 K (c) and at 290 K (d).

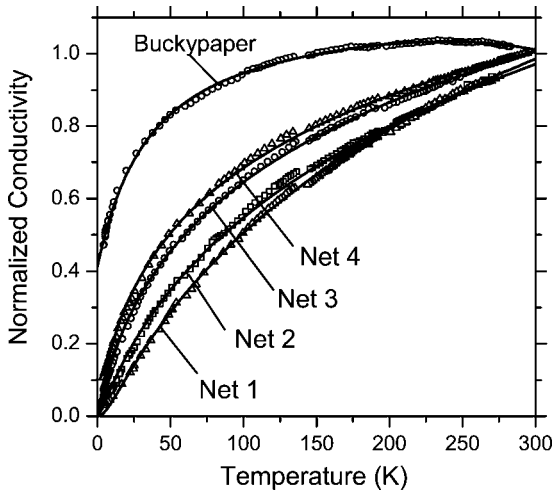

FIG. 10. Temperature dependences of the electrical conductance of SWNT freestanding film and four thin networks normalized to their values at room temperature $\sigma(T)/\sigma(292\ \mathrm{K})$; the full lines are fits to the variable-range hopping expression Eq. (5) for the networks, and to the interrupted metallic model Eq. (4) for freestanding film.

crease in conductivity due to scattering of carriers by phonons may dominate the T dependence, leading to the peak in conductance often observed in highly conducting polymers and SWNT networks.[28,36,37] It was proposed long ago[38] that the conductance peak seen in polycrystalline graphite samples (not in monocrystals) near 670 K (Ref. 39) could arise from the number of charge carriers increasing with temperature due to the special density of states of graphite,[40] combined with phonon scattering that gives the dominant effect at high temperatures. The peak was associated with the presence of grain boundaries in that the large temperature-independent scattering from the grain boundaries dominated the resistance at low temperatures, allowing the observation of the increase of conductance due to the increase of charge carriers with temperature.

We suggest that for our thick SWNT networks, the main contribution to the metalliclike behavior of the conductivity with temperature (a negative sign of the slope) of the thick freestanding film at the temperatures above 240 K arises from zone boundary in-plane phonon scattering, in analogy to an earlier suggestion for the field dependence of conductance for an individual SWNT with a very low contact resistance.[41] We write the expression for conductance $G(T)$ in the form[30]

$$\frac{1}{G(T)} = A\exp\left(-\frac{T_m}{T}\right) + B\exp\left(\frac{T_b}{T_s+T}\right), \tag{4}$$

where the geometrical factors A and B can be taken as constant. The first term is for quasi-one-dimensional metallic conduction involving suppression of resistivity at lower temperatures where carriers are not easily backscattered (for scattering by lattice vibrations $k_B T_m$ would be the energy of the backscattering $2k_F$ phonons,[42] where k_F is the Fermi wave vector). The second term represents fluctuation-assisted tunneling[43] through barriers, with the order of magnitude of typical barrier energies indicated by the value of $k_B T_b$ and the extent of the decrease of conductivity at low temperatures is indicated by the ratio T_s/T_b. For the present we neglect any expansion effects and take T_b as independent of temperature.

As discussed in our earlier paper,[28] this expression [Eq. (4)] gave a very good description of the conductance T dependence for the thick network, and still described the conductance data well when the free carrier density was increased or decreased by different chemical treatments, although the metallic characteristics were strongly reduced when the treatment lowered the carrier density.[28] In the present fit we varied the value of T_m to achieve the best fit to the freestanding film data in Fig. 10, obtaining a value of 1830 K (corresponding to 160 meV or 1230 cm^{-1}). This value agrees with the band of energies $1000-2000\mathrm{cm}^{-1}$ expected for the in-plane zone boundary phonons in a SWNT.[44,41] This agreement leads us to suggest that it is backscattering by these phonons that causes the turnover to metallic sign of the conductivity T dependence for the freestanding film sample. We note that in a complementary experiment investigating the dependence of conductance on bias voltage rather than temperature, Yao *et al.*[41] found that optical and zone boundary phonons played the major role in limiting the conductance as bias voltage reached large values for SWNTs with low-resistance electrode contacts.

The mechanism of scattering of charge carriers by zone boundary phonons we have discussed above is an intrinsic process in each individual SWNT. A secondary effect causing a decrease of conductivity at higher temperatures could arise from transport between the SWNTs, namely decreasing probability of electron tunneling between the tubes at the crossings of the SWNTs in the network. This effect is suggested by investigations of the temperature dependence of the radial breathing mode (RBM) studied by Raman spectroscopy.[45] Based on experimental data and the results of molecular dynamics simulations, a softening of the van der Waals intertubular interactions in SWNT bundles was found. In the directions perpendicular to the tube axis (but not in the parallel direction), SWNT bundles exhibit a large thermal expansion coefficient with a value of $\alpha = 0.75\times10^{-5}/\mathrm{K}$. This could lead to lessening of intertube transfer of carriers at higher temperatures in the thick networks.

The situation is rather different, however, for the conductivity of the four very thin networks shown in Fig. 10: the metallic characteristics are essentially eliminated, with the conductivity extrapolating to almost zero in the zero-temperature limit, and with no sign of a changeover to metallic temperature dependence at higher temperatures. In fact, the conductivity continues to increase near room temperature in a rather linear fashion that does not agree well with the interrupted metallic conduction expression, Eq. (4). As shown by the fits in Fig. 10, these thin network data show behavior closer to that for variable-range hopping (VRH):[46]

$$\sigma(T) = \sigma_0 \exp\left[-\left(\frac{T_0}{T}\right)^{1/(1+d)}\right], \tag{5}$$

where σ_0 and T_0 are constants and d is the dimensionality of the hopping conduction ($d=3$ for Nets 2, 3, and 4, and $d=2$ for Net 1).

We ascribe the change to hopping-type conduction as the networks become thin to the greater difficulty of achieving good metallic percolation paths through the samples as the sample thickness is reduced, as indicated by the dramatically reduced conductance shown in Fig. 7, especially in the thinnest network (Net 1). This interpretation is also supported by our observation that Net 1 gives slightly better agreement with the VRH expression for dimensionality $d=2$, whereas the others agree better with the $d=3$ expression (the better agreement with $d=2$ and 3 than with $d=1$ suggests that in each case the greatest resistance is associated with hopping between tubes rather than along a single tube). We note that Bekyarova *et al.*[47] found good agreement with our Eq. (4) without a significant temperature-dependent metallic term for the temperature-dependent resistivity of their thicker as-prepared and purified SWNTs. Their thinner films also showed a greater decrease in normalized conductance as temperature decreased but the functional form was not analyzed.

C. Individual MWNTs

We have also made measurements on individual multiwall carbon nanotubes to compare with those on individual SWNTs and bundles of SWNTs. In contrast to SWNT bundles, the nanotubes in MWNTs are concentric and of larger diameter. Figure 11 shows the temperature dependence of the electrical conductance $G(T)$ and the I-V characteristics of similar individual MWNTs of diameter approximately 40 nm. The most striking feature is that individual MWNTs show much more metallic character than SWNTs, and more metallic even than bundles of SWNTs: the conductance extrapolates to large nonzero values at zero temperature (only about 25% less than the room-temperature conductance), and the I-V characteristics are closely linear down to helium temperatures. One of our MWNTs did show a greater decrease of conductance as temperature decreased similar to that measured by Song *et al.*[14] (but still showing metallic behavior as conductance did not approach zero at helium temperatures). Ebbesen *et al.*[13] found a decrease in conductance as temperature decreased, but for most of their MWNTs the decrease was more linear than our MWNTs in Fig. 11(a) and the conductance at helium temperature was only about 10% less than the room-temperature conductance.

Despite the metallic character indicated by the retention of substantial conductance at very low temperatures, the temperature dependence of conductance shows a nonmetallic positive sign up to room temperature. This is not unexpected since intershell transfer and the much larger diameter of our MWNTs compared to the SWNTs will lessen the importance of the quasi-one-dimensional suppression of backscattering in Eq. (4). In addition, in a MWNT, the thermal expansion in the directions perpendicular to the tube axis is strictly limited by the expanded diameter of the outermost shell of the MWNT for a particular temperature, and therefore, there is no reason to expect an increase of the tunneling barrier between the shells as we postulated for SWNT bundles due to softening of the van der Waals intertubular interactions.

The mixed metallic/nonmetallic behavior is somewhat similar to that often seen in highly conducting polymers or

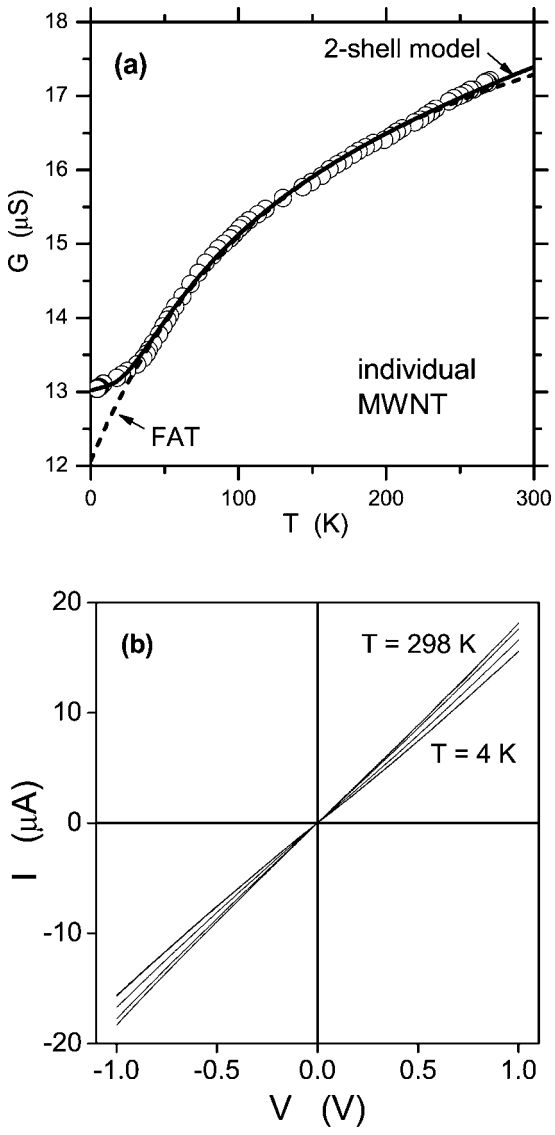

FIG. 11. (a) Temperature dependence of the electrical conductance of an individual multiwall nanotube MWNT-1 fitted to Eq. (7) for our simple model of conduction in the two outer shells (full line) and to Eq. (6) with $R_m=0$ for fluctuation-assisted tunneling (FAT) alone (dashed line); for clarity only a third of the data points are plotted. (b) I_D-V_{DS} characteristics for a similar individual MWNT-2 to the tube MWNT-1 (the conductance values for MWNT-2 from this I_D-V_{DS} plot are within 8% of those for MWNT-1 at all temperatures).

SWNT networks, suggesting that a model of interrupted metallic conduction may also be applicable to MWNTs. If we take the total resistance of the metallic highly conducting portions of the conducting path as R_m, and consider fluctuation-assisted tunneling though barriers as limiting the conductance, the expression for conductance $G(T)$ has the form

$$\frac{1}{G(T)} = R_m + B\exp\left(\frac{T_b}{T_s + T}\right), \tag{6}$$

where the other parameters are the same as in Eq. (4). Taking the metallic resistance R_m of the defect-free portions of the

MWNT as negligible, the fit in Fig. 11(a) to the second term of Eq. (6) alone shows that the nonmetallic increase of conductance with temperature for the MWNT is generally consistent with that expected for fluctuation-assisted tunneling, but the reduced gradient of the data below 40 K is not accounted for by this model. A reduction in gradient, or even an upturn in conductivity at low temperatures, is seen in highly conducting polypyrrole, other conducting polymers and disordered metals, and can be explained by electron-electron interaction effects.[36] However, in view of the finding by Bourlon *et al.*[16] that the second shell plays a significant role in conduction in MWNTs with side contacts to electrodes, we propose the following interpretation of our MWNT data.

The sharp increase in conductance above 40 K is a key feature of our MWNT data. We suggest this sharp increase could be due to the onset of thermally assisted transfer of electrons from the outer shell to the second shell. We take the conductance of the outer shell between the voltage electrodes as G_1, and the current through the second shell as having a term increasing according to activated or fluctuation-assisted tunneling behavior.[43] This additional current in parallel then yields an increase in measured conductance of the form

$$G(T) = G_1 + G_{20} \exp\left(-\frac{T_b}{T_s + T}\right). \tag{7}$$

We take $G_1 = G_{10} + AT$ to incorporate a term increasing linearly with temperature T, as suggested by the data of Ebbesen *et al.*[13] and our high-temperature data. A conductance increasing linearly with T would be expected for a graphene sheet behaving as a zero-gap semiconductor[40] (neglecting the T dependence of the mean free path). It can be seen that this simple two-shell model gives a good account of our data in Fig. 11(a). The fitted value of the activation energy $k_B T$ was 7.3 meV ($T_b = 85$ K), and the other parameter values were $G_{10} = 13.0\ \mu$S, $A = 5.3 \times 10^{-3}\ \mu$S/K and $G_{20} = 3.7\ \mu$S. The parameter T_s was zero, i.e., a simple activated form was adequate to describe the nonlinear temperature dependence. Of course, these temperature-dependent conductance terms account for only 25% of the total conductance at room temperature so conduction by most charge carriers shows little temperature dependence.

IV. CONCLUSIONS

We have investigated the evolution of the electronic transport properties of carbon nanotube materials, starting with individual SWNTs and bundles of SWNTs, progressing to SWNT networks of varying thickness, and finishing with individual MWNTs for comparison. Our key conclusions are:

(i) Our data for metallic SWNTs are consistent with tunneling through an interfacial barrier into a Luttinger liquid, where the intrinsic barrier transmission probability is assumed to be energy independent and the power-law temperature dependence arises from the suppression of the tunneling density of states near the Fermi level in the m-SWNT (or an environmental Coulomb blockade model giving equivalent behavior). However, we also find evidence for activated behavior with barrier energies of approximately 5 meV as found by Hunger *et al.*[33] in metallic thick SWNT bundles but in our case independent of drain-source voltage.

(ii) The thinnest SWNT networks, like the individual semiconducting SWNTs, show nonlinear *I-V* characteristics at low temperatures with a current that can be modulated by a gate voltage. Schottky barriers found in individual semiconducting SWNTs are expected to control the electron transport in the thinnest SWNT networks. Such networks therefore show promise for applications in devices. In contrast, thick freestanding SWNT networks show linear *I-V* characteristics with no gate-voltage effect.

(iii) The conductance of our thin SWNT networks becomes very small as zero temperature is approached. There is a systematic change in the shape of the temperature dependence of conductance as the thickness of the network increases, but the overall temperature dependence in all four thin networks is consistent with hopping conduction as seen in disordered semiconductors. On the other hand, the conductance of the thickest SWNT network, a freestanding film, is much more metallic, retaining a large fraction of its conductance to very low temperatures. For this thick network, the conductance reaches a maximum value near room temperature with a changeover to metallic temperature dependence at higher temperatures. This temperature dependence is consistent with fluctuation-assisted tunneling through thin barriers separating metallic regions with reduction of the conductivity at higher temperatures as backscattering by phonons increases. We obtain an excellent fit to the data taking the energy of the backscattering phonons as 160 meV, in good agreement with the energies of the $2k_F$ zone boundary phonons in SWNTs. We therefore propose that backscattering by these phonons is the cause of the changeover to metallic sign for the conductivity near 230 K.

(iv) We have also proposed another mechanism that could lead to reduction of the conductance in SWNT networks at higher temperatures, namely the relatively large expansion of the diameter of SWNT bundles due to the softening of the van der Waals intertubular interactions, which leads to a reduction in intertube transfer of carriers.

(v) Individual MWNTs, which in some ways represent individual tubes combined as coaxial "networks," show weak temperature dependence in some cases, with even greater retention of conductance to very low temperatures than thick SWNT networks. However, there is no changeover to metallic temperature dependence for the conductance up to room temperature. We have shown that the sharp increase in conductance around 40 K that we observe can be accounted for by a model in which conduction through the outer shell of the MWNT is dominant, but thermally assisted tunneling to the second outermost shell also contributes to electron transport in the MWNT.

For the same reason as mentioned in (iii), we note that if the "interlayer" interaction is weaker at high temperatures, MWNTs grown at high temperatures of 600 °C or more would tend to be created with intershell spacings larger than those corresponding to room temperature. Since the thermal expansion of the tubes themselves is very small, this larger separation would tend to be retained once the MWNT was cooled to lower temperatures and electronic transfer between shells would be impeded. In fact, intertube separations in

double-wall carbon nanotubes (DWNTs) created at 1300 °C do average 0.36 nm,[48] larger than the spacing of the layers in turbostratic graphite, but similar large separations have been associated with the high curvature of the shells.[49]

ACKNOWLEDGMENTS

This work was supported by EU projects SPANK, INKONAMI, CANAPE. V.S. thanks Martti Kaempgen for SWNT network preparation.

*Electronic address: V.Skakalova@fkf.mpg.de

[1] R. Saito, G. Dresselhaus, and M. S. Dressselhaus, *Physical Properties of Carbon Nanotubes* (Imperial College Press, London, 1998).
[2] S. Roth and D. Carroll, *One-Dimensional Metals* (Wiley-VCH, Weinheim, 2004).
[3] S. Reich, C. Thomsen, and J. Maultzsch, *Carbon Nanotubes: Basic Concepts and Physical Principles* (Wiley-VCH, Weinheim, 2004).
[4] S. J. Tans, M. H. Devoret, H. Dai, A. Thess, R. E. Smalley, L. J. Geerligs, and C. Dekker, Nature **386**, 474 (1997).
[5] A. Javey, J. Guo, Q. Wang, M. Lundstrom, and H. Dai, Nature **424**, 654 (2003).
[6] M. Bockrath, D. H. Cobden, P. L. McEuen, N. G. Chopra, A. Zettl, A. Thess, and R. E. Smalley, Science **275**, 1922 (1997).
[7] M. Bockrath, D. H. Cobden, J. Lu, A. G. Rinzler, R. E. Smalley, L. Balents, and P. L. McEuen, Nature **397**, 598 (1999).
[8] Z. Yao, H. W. Ch. Postma, L. Balents, and C. Dekker, Nature **402**, 273 (1999).
[9] F. Leonard and J. Tersoff, Phys. Rev. Lett. **84**, 4693 (2000).
[10] S. Heinze, J. Tersoff, R. Martel, V. Derycke, J. Appenzeller, and Ph. Avouris, Phys. Rev. Lett. **89**, 106801 (2002).
[11] R. Martel, T. Schmidt, H. R. Shea, T. Hertel, and Ph. Avouris, Appl. Phys. Lett. **73**, 2447 (1998).
[12] S. J. Tans, A. R. M. Verschueren, and C. Dekker, Nature **393**, 49 (1998).
[13] T. W. Ebbesen, H. J. Lezec, H. Hiura, J. W. Bennett, H. F. Ghaemi, and T. Thio, Nature (London) **382**, 54 (1996).
[14] S. N. Song, X. K. Wang, R. P. H. Chang, and J. B. Ketterson, Phys. Rev. Lett. **72**, 697 (1994).
[15] A. Bachtold, C. Strunk, J.-P. Salvetat, J.-M. Bonard, L. Forró, T. Nussbaumer, and C. Schönenberger, Nature **397**, 673 (1999).
[16] B. Bourlon, C. Miko, L. Forró, D. C. Glattli, and A. Bachtold, Phys. Rev. Lett. **93**, 176806 (2004).
[17] C. Schönenberger, A. Bachtold, C. Strunk, J.-P. Salvetat, and L. Forró, Appl. Phys. A: Mater. Sci. Process. **69**, 283 (1999).
[18] R. Egger and A. O. Gogolin, Phys. Rev. Lett. **87**, 066401 (2001).
[19] T. Kanbara, T. Iwasa, K. Tsukagoshi, Y. Aoyagi, and Y. Iwasa, Appl. Phys. Lett. **85**, 6404 (2004).
[20] T. Kanbara, K. Tsukagoshi, Y. Aoyagi, and Y. Iwasa, AIP Conf. Proc. **786**, 499 (2005).
[21] H. J. Li, W. G. Lu, J. J. Li, X. D. Bai, and C. Z. Gu, Phys. Rev. Lett. **95**, 086601 (2005).
[22] E. Artukovic, M. Kaempgen, D. S. Hecht, S. Roth, and G. Grüner, Nano Lett. **5**, 757 (2005).
[23] Z. Wu, Z. Chen, X. Du, J. M. Logan, J. Sippel, M. Nikolou, K. Kamaras, J. R. Reynolds, D. B. Tanner, A. F. Hebard, and A. Rinzler, Science **305**, 1273 (2004).
[24] N. Chakrapani, J. M. Zhang, S. K. Nayak, J. A. Moore, D. L. Carroll, Y. Y. Choi, and P. M. Ajayan, J. Phys. Chem. B **107**, 9308 (2003).
[25] E. S. Snow, F. K. Perkins, E. J. Houser, S. C. Badescu, and T. L. Reinecke, Science **307**, 1942 (2005).
[26] J. P. Novak, E. S. Snow, E. J. Houser, D. Park, J. L. Stepnowski, and R. A. McGill, Appl. Phys. Lett. **83**, 4026 (2003).
[27] A. Goldoni, R. Larciprete, L. Petaccia, and S. Lizzit, J. Am. Chem. Soc. **125**, 11329 (2003).
[28] V. Skákalová, A. B. Kaiser, U. Dettlaff-Weglikowska, K. Hrnčariková, and S. Roth, J. Phys. Chem. B **109**, 7174 (2005).
[29] A. B. Kaiser, G. Düsberg, and S. Roth, Phys. Rev. B **57**, 1418 (1998).
[30] A. B. Kaiser, Rep. Prog. Phys. **64**, 1 (2001).
[31] J. C. Meyer, D. Obergfell, S. Roth, S. Yang, and S. Yang, Appl. Phys. Lett. **85**, 2911 (2004).
[32] R. Seidel, M. Liebau, G. S. Duesberg, F. Kreupl, E. Unger, A. P. Graham, and W. Hoenlein, Nano Lett. **3**, 965 (2003).
[33] Th. Hunger, B. Lengeler, and J. Appenzeller, Phys. Rev. B **69**, 195406 (2004).
[34] C. Kane, L. Balents, and M. P. A. Fisher, Phys. Rev. Lett. **79**, 5086 (1998).
[35] R. Martel, V. Derycke, C. Lavoie, J. Appenzeller, K. K. Chan, J. Tersoff, and Ph. Avouris, Phys. Rev. Lett. **87**, 256805 (2001).
[36] A. B. Kaiser, Adv. Mater. (Weinheim, Ger.) **13**, 927 (2001).
[37] P. Fedorko, D. Djurado, M. Trznadel, B. Dufour, P. Rannou, and J. P. Travers, Synth. Met. **135-136**, 327 (2003).
[38] D. Bowen, Phys. Rev. **76**, 1878 (1949).
[39] L. J. Collier, W. S. Stiles, and W. G. A. Taylor, Proc. Phys. Soc. (London) **51**, 147 (1939).
[40] P. R. Wallace, Phys. Rev. **71**, 622 (1947).
[41] Z. Yao, C. L. Kane, and C. Dekker, Phys. Rev. Lett. **84**, 2941 (2000).
[42] L. Pietronero, Synth. Met. **8**, 225 (1983).
[43] P. Sheng, Phys. Rev. B **21**, 2180 (1980).
[44] M. S. Dresselhaus, G. Dresselhaus, and P. C. Eklund, *Science of Fullerenes and Carbon Nanotubes* (Academic, San Diego, 1996).
[45] N. R. Raravikar, P. Keblinski, A. M. Rao, M. S. Dresselhaus, L. S. Schadler, and P. M. Ajayan, Phys. Rev. B **66**, 235424 (2002).
[46] N. F. Mott and E. A. Davis, *Electronic Processes in Non-Crystalline Materials*, 2nd ed. (Clarendon, Oxford, 1979).
[47] E. Bekyarova, M. E. Itkis, N. Cabrera, B. Zhao, A. Yu, J. Gao, and R. C. Haddon, J. Am. Chem. Soc. **127**, 5990 (2005).
[48] R. Pfeiffer, H. Kuzmany, Ch. Kramberger, Ch. Schaman, T. Pichler, H. Kataura, Y. Achiba, J. Kurti, and V. Zolyomi, Phys. Rev. Lett. **90**, 225501 (2003).
[49] C.-H. Kiang, M. Endo, P. M. Ajayan, G. Dresselhaus, and M. S. Dresselhaus, Phys. Rev. Lett. **81**, 1869 (1998).